Supplementary Information

Note S1: The photon-to-photon conversion efficiency η_{p-p} is the sum of the visible light output efficiency for each cycle. The ratio of the efficiency of the (n+1)th output to the (n)th output is $\alpha\eta_{PSL}\eta_{EML}$, meaning that the decay rate of the output light efficiency per cycle is a fixed value. Therefore, η_{p-p} can be calculated using the following geometric series summation formula, where the common ratio is $\alpha\eta_{PSL}\eta_{EML}$:

$$\eta_{p-p} = (1-\alpha)\eta_o\eta_A\eta_{PSL}\eta_{EML} + (1-\alpha)\eta_o\eta_A\eta_{PSL}\eta_{EML} \times \alpha\eta_{PSL}\eta_{EML} + (1-\alpha)\eta_o\eta_A\eta_{PS}$$
$$]^2 + \cdots + S_n = \frac{(1-\alpha)\eta_o\eta_A\eta_{PSL}\eta_{EML}}{1-\alpha\eta_{PSL}\eta_{EML}}$$

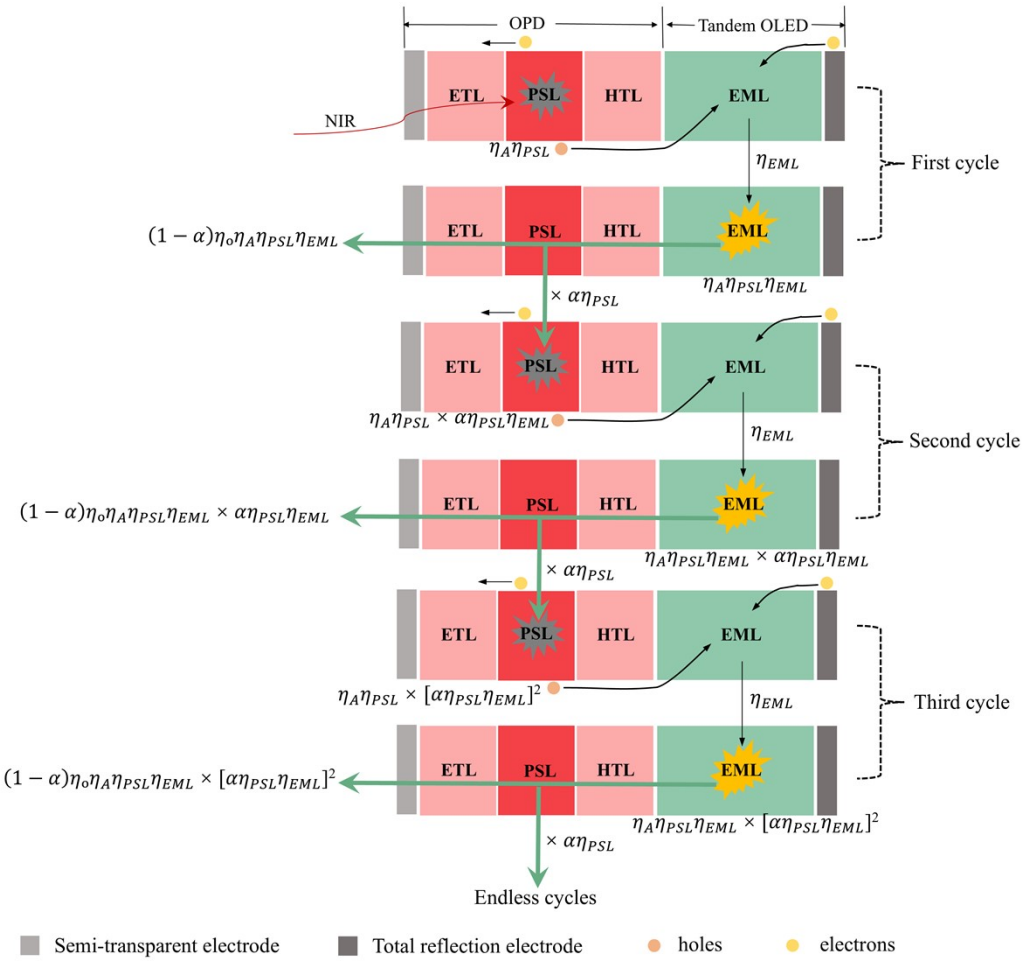

Figure S1 Schematic diagram of the process of photons and charge carrier recycling within the device.

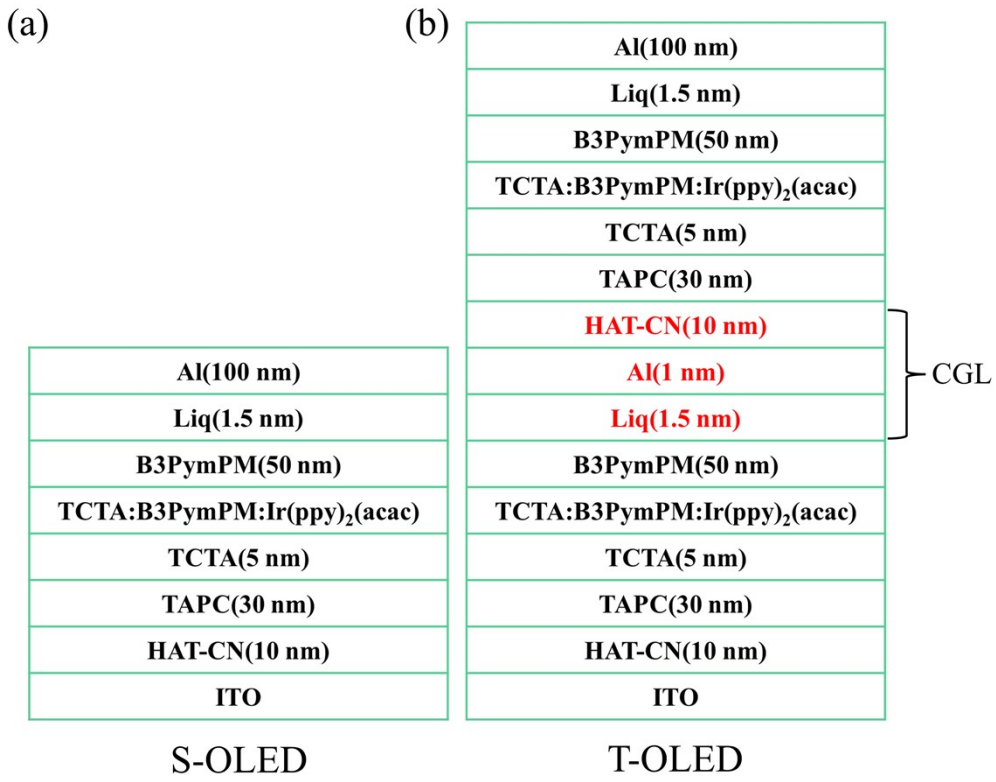

Figure S2 Detailed structures of (a) S-OLED and (b)T-OLED.

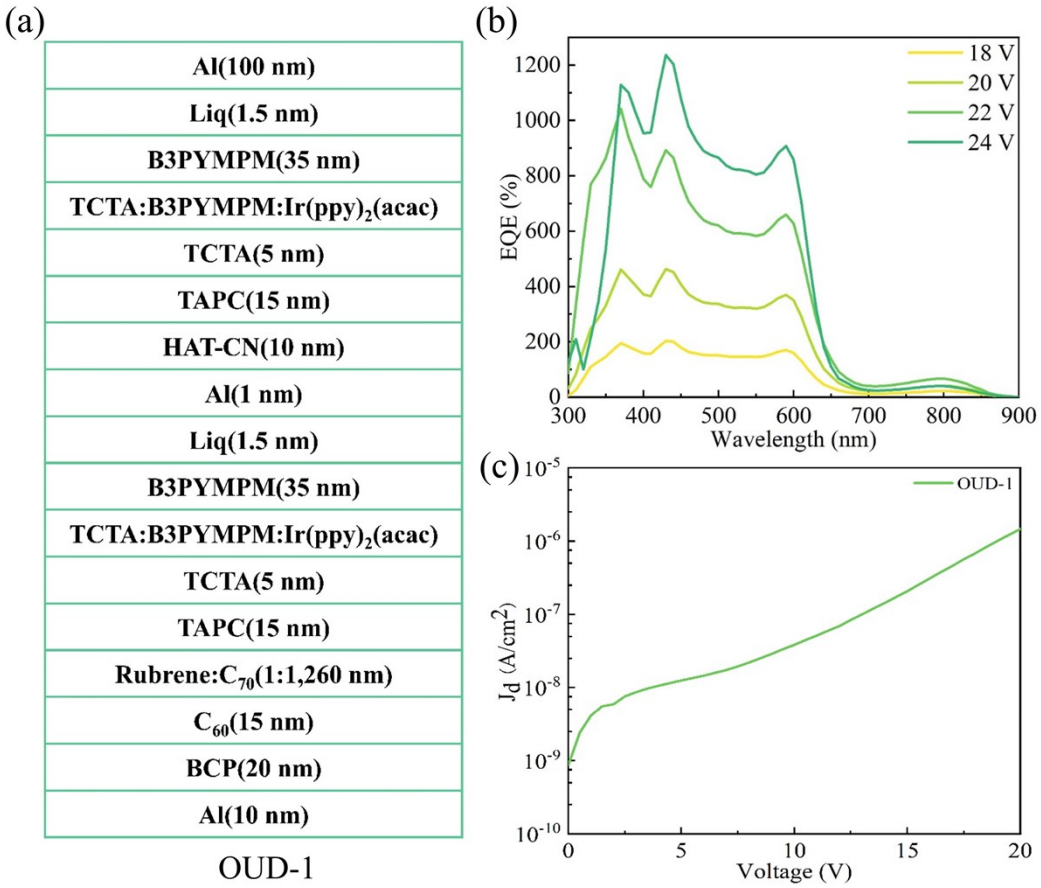

Figure S3 (a) Detailed structure of OUD-1. (b) *EQE* spectra. (c) Dark current density-voltage curve.

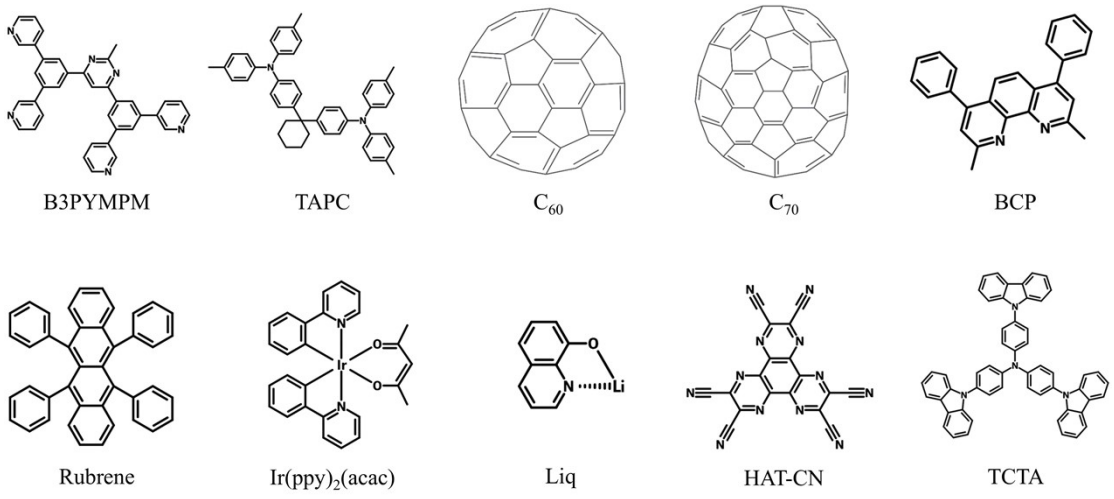

Figure S4 Chemical structures of the used organic materials.

Note S2: We conducted a 60-minute comparative operational stress test on encapsulated and unencapsulated OUD-2 devices under a continuous 20 V bias. Under unencapsulated conditions, the device suffered rapid degradation from moisture and oxygen, resulting in extremely low initial photocurrent density and luminance, followed by swift decay. With encapsulation, the device successfully maintained its high initial performance and showed vastly superior stability. The moderate decay observed in the encapsulated device over time is primarily attributed to the intrinsic electrical aging of the OLED emissive units under high-voltage continuous driving, rather than environmental degradation. This confirms the functional viability of the device and highlights its potential for practical applications.

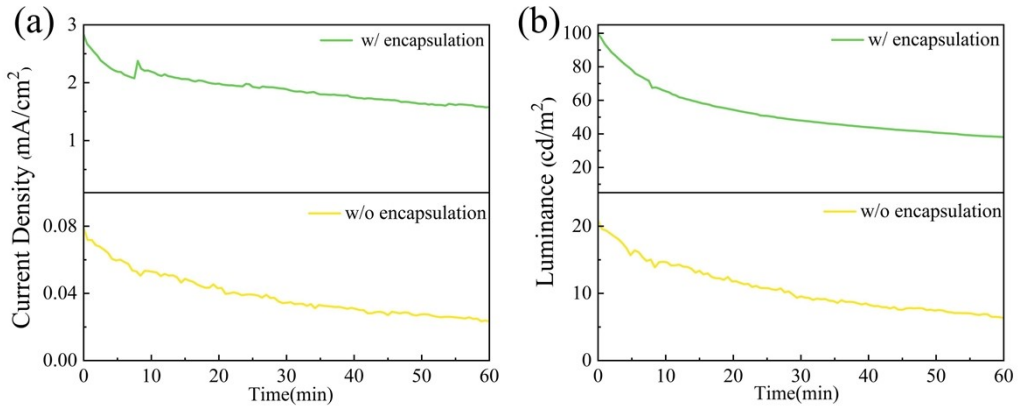

Figure S5 Decay curves of (a) photocurrent density and (b) luminance over time for encapsulated and unencapsulated OUD-2 devices under a 20 V bias for 60 minutes (laser intensity: 0.11 mW/cm^2, wavelength: 780 nm).

Note S3：We evaluated the transient photocurrent response of OUD-2. The rise time (τ_r) and fall time (τ_f) were measured to be 5.9 ms and 4.4 ms, respectively. A comparison with previously reported data in the literature is summarized in Table S1. The response

speed is highly dependent on the operational mechanism; photomultiplication-type devices generally exhibit slower responses, whereas direct carrier-injection devices are faster. Our device demonstrates a moderate and competitive response speed suitable for practical imaging.

Table S1 Summary of response times for up-conversion device

Infrared photoactive system	Visible light-emitting system	Photocurrent response (τ_r/τ_f)	Test Conditions	[Ref.]
PCBM:DCSQ1 (980 nm)	CzDBA (575 nm)	25 ms, 70 ms	980 nm@-10 V, 25.3 mW/cm^2	[1]
ClAlPc (780 nm)	BCzPh:CN-T2T: $Ir(ppy)_2(acac)$ (520 nm)	563.56μs, 302.4 μs	780 nm@10 V, 1.0 mW/cm^2	[2]
DPP-DTT: CO_i8DFIC (850 nm)	$CsPbBr_3$ (520 nm)	76 μs, none	780 nm@3 V, 2 kHz frequency-modulated	[3]
$FAPbI_3$ (830 nm)	CBP:$Ir(ppy)_2(acac)$ (520 nm)	10 μs, 43 μs	810 nm@5 V, 1 kHz frequency-modulated	[4]
PbS-I QDs (940 nm)	$Bepp_2$:$Ir(ppy)_2acac$ (560 nm)	0.866 ms, none	810 nm@28 V, 0.443 mW/cm^2	[5]
PbS CQDs (940 nm)	CdSe/ZnS QDs (525 nm)	1 ms, 1.5 ms	940 nm@6 V, 10 mW/cm^2	[6]
SubPc/ClAlPc:C_{70} (750 nm)	TCTA:$Ir(ppy)_3$/ CBP:$Ir(ppy)_3$ (570 nm)	10 ms, none	750 nm@14 V, 30 μW/cm^2	[7]
Rubrene:C_{70} (780 nm)	TCTA:B3PYMPM: $Ir(ppy)_2(acac)$ (570 nm)	5.9 ms, 4.4 ms	780 nm@20 V, 0.11 mW/cm^2	This work

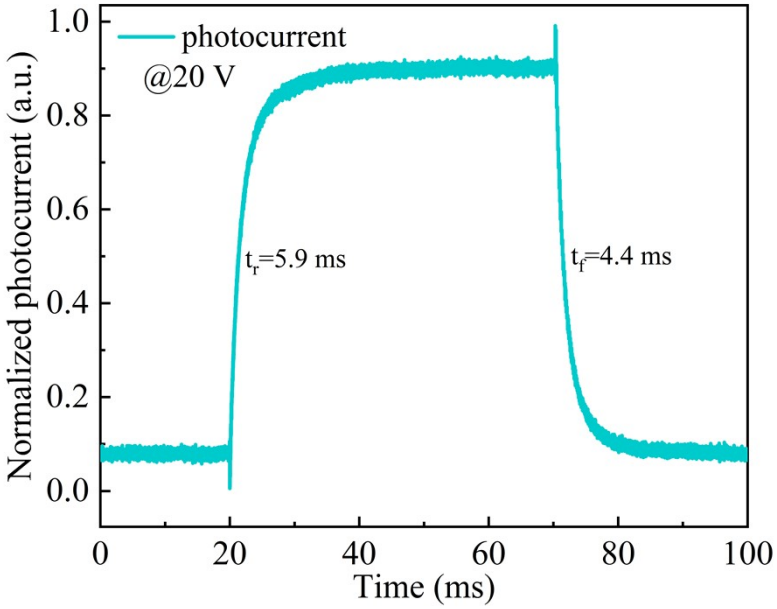

Figure S6 Testing the transient photocurrent response of the OUD-2 at a 20 V bias using near-infrared light at 780 nm and 0.11 mW/cm^2.

References:

[1] W.-H. Hu, J. P. F. Assunção, R. dos S. Carvalho, E. Didier, M. Diethelm, S. Jenatsch, D. Bachmann, I. Shorubalko, M. Cremona, F. Nüesch, M. Bauer, R. Hany, *Adv. Funct. Mater.* **2024**, *34*, 2407528.

[2] C.-J. Shih, C.-Y. Lin, K. Chen, N. R. A. Amin, D. Luo, I.-S. Hsu, A. K. Akbar, S. Biring, C.-H. Lu, B.-H. Chen, S.-D. Yang, J.-H. Lee, S.-W. Liu, *Adv. Sci.* **2023**, *10*, 2302631.

[3] N. Li, Y. S. Lau, Z. Xiao, L. Ding, F. Zhu, *Adv. Opt. Mater.* **2018**, *6*, 1801084.

[4] B. H. Yu, Y. Cheng, M. Li, S.-W. Tsang, F. So, *ACS Appl. Mater. Interfaces* **2018**, *10*, 15920.

[5] J. H. Kim, J.-Y. Lee, C. Lim, J. Roh, S.-W. Baek, W. Kim, M. C. Suh, H. Yu, *Adv. Funct. Mater.* **2023**, *33*, 2214530.

[6] W. Zhou, Y. Shang, F. P. García De Arquer, K. Xu, R. Wang, S. Luo, X. Xiao, X. Zhou, R. Huang, E. H. Sargent, Z. Ning, *Nat. Electron.* **2020**, *3*, 251.

[7] R. Lampande, J.-P. S. DesOrmeaux, A. Pizano, J. R. Schrecengost, R. Cawthorn, H. Bowman, A. Grede, U. Guler, J. W. Hamer, N. C. Giebink, *Nat. Photonics* **2024**, 1.